Fine-structure mixing in 7^2D and 8^2D Rb atoms, induced in collisions with ground-state atoms and molecules

J. Supronowicz, J. B. Atkinson, and L. Krause
Department of Physics, University of Windsor, Windsor, Ontario, Canada N9B 3P4
(Received 14 October 1983)

Cross sections for 7^2D and 8^2D fine-structure mixing in Rb, induced by collisions with various ground-state atoms and N_2 molecules, have been determined using methods of atomic fluorescence. Rb vapor, pure or mixed with a buffer gas, was irradiated in a glass fluorescence cell with pulses of radiation from a N_2 laser-pumped dye laser, populating a ^2D fine-structure state by two-photon absorption. The resulting fluorescence included a direct component arising from the optically excited state and a sensitized component due to the collisionally populated fine-structure state. Measurements of relative intensities of the two components in relation to buffer-gas pressure yielded the following cross sections (in units of 10^{-14} cm^2): $Q(7^2D_{3/2}\rightarrow 7^2D_{5/2})=14.1$, 15.5, and 10.0; $Q(7^2D_{3/2}\leftarrow 7^2D_{5/2})=9.0$, 10.5, and 6.9, for Kr, Xe, and N_2, respectively; $Q(8^2D_{3/2}\rightarrow 8^2D_{5/2})=8.9$, 4.9, 12.4, 24.9, 25.8, 12.1, and 43.1; $Q(8^2D_{3/2}\leftarrow 8^2D_{5/2})=5.8$, 3.2, 9.4, 15.1, 17.6, 8.3, and 28.5, for He, Ne, Ar, Kr, Xe, N_2, and Rb, respectively. Cross sections for the effective depopulation of the ^2D states were also determined.

I. INTRODUCTION

Collisional excitation transfer (fine-structure mixing) and quenching in alkali atoms excited to ^2P resonance states have been investigated experimentally for many years using vapor cells and spectroscopic methods[1] and have recently been reexamined using atomic-beam techniques.[2] In recent years there has also been a large number of investigations of collisional interactions involving alkali atoms in high "Rydberg" states. In sodium such processes were studied by Gallagher *et al.*[3] and by Biraben *et al.*,[4] and in rubidium by Hugon *et al.*[5] These experimental studies have been paralleled by theoretical calculations dealing with interactions of atoms in resonance[6] and Rydberg[7,8] states.

There have been comparatively few experiments and no theoretical treatments concerned with collisions of atoms excited to "intermediate" states lying above the resonance levels but not classified as true Rydberg states, which are not amenable to calculations based on the "free-electron" model.[8] Fine-structure mixing experiments have been reported, involving n^2D Rb atoms colliding with ground-state Rb atoms, for $n=5$–9.[9–11] Noble-gas collisions were also employed to induce 6^2D mixing[12] and 7^2D mixing in Rb.[10] A determination of depopulation cross sections for Na ns states ($n=5$–11) colliding with H_2 and CO molecules was recently carried out by Gallagher *et al.*,[13] and experiments with N_2 were performed in the same laboratory some years earlier.[14]

We present here the results of experiments in which we investigated fine-structure mixing in 7^2D and 8^2D Rb atoms, induced in collisions with noble-gas atoms and N_2 molecules. We have also remeasured the cross sections for Rb-Rb collisional $8^2D_{3/2}$-$8^2D_{5/2}$ transfer, which supersede the previous values of Głódź *et al.*[9]

II. EXCITATION AND DECAY PROCESSES

An energy-level diagram showing the states involved in the experiments and the transitions between them is shown in Fig. 1. The Rb atoms are selectively excited by two-photon absorption to one of the 7^2D or 8^2D fine-structure substates, which can decay to the $5^2P_{1/2}$ or $5^2P_{3/2}$ state, emitting direct fluorescence, or be collisionally transferred to the other ^2D substate whose decay gives rise to sensitized fluorescence. Inelastic collisions of ^2D atoms may also result in transfers to lower-energy states (including the ground state), causing depopulation of the ^2D states. The collisional fine-structure mixing processes may be represented as follows:

$$\mathrm{Rb}(n\,^2D_{5/2})+A\leftrightarrow\mathrm{Rb}(n\,^2D_{3/2})+A+\Delta E\ , \qquad (1)$$

where A denotes a buffer-gas atom or molecule, or a ground-state Rb atom, and ΔE represents the appropriate fine-structure splitting between the ^2D states.

Figure 1 also shows the various fluorescent components

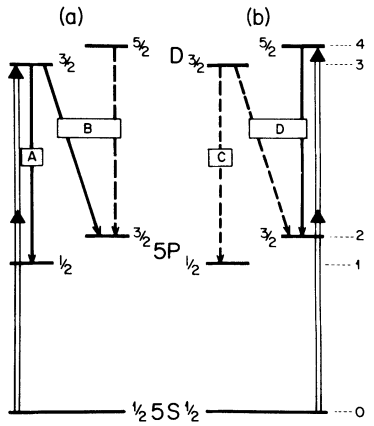

FIG. 1. Energy-level diagram of the Rb states involved in the two-photon absorption and fluorescent emission processes. (a) indicates the transitions taking place when a $^2D_{3/2}$ state is optically excited; (b) corresponds to optical excitation of a $^2D_{5/2}$ state (diagram not to scale). The observed fluorescent components are labeled *A*, *B*, *C*, *D*.

TABLE I. Ratios of Einstein A coefficients.

Rb state	A_{31}/A_{42}	A_{32}/A_{31}
7^2D	0.7985	0.2106
8^2D	0.8000	0.2100

that are observed in the experiment, bearing in mind that a $D_{3/2}$ state may decay to the $5^2P_{1/2}$ or $5^2P_{3/2}$ state, but a $D_{5/2}$ state may decay only to the $5^2P_{3/2}$ state. Since the available spectrometer could not resolve the ^2D fine-structure splitting which is of the order of 1 cm^{-1}, the observed fluorescent spectrum always consisted of two components. When the $^2D_{3/2}$ state was optically excited, the component A was due to direct fluorescence and component B to a mixture of direct and sensitized fluorescence. When, on the other hand, $^2D_{5/2}$ was the primarily populated state, the fluorescent component C was due entirely to sensitized fluorescence and D to a mixture of direct and sensitized fluorescence.

It may be shown that measurements of time-integrated intensities of the observed fluorescent components yield the ^2D fine-structure mixing and depopulation cross sections[10]

$$\frac{1}{I_B/I_A-(A_{32}/A_{31})}=\frac{A_{31}}{A_{42}}\frac{1}{\tau_4 Q_{34}}\frac{1}{N_0 v}+\frac{A_{31}}{A_{42}}\frac{Q_{43}+Q_4}{Q_{34}}, \tag{2}$$

$$\frac{I_D}{I_C}=\frac{A_{42}}{A_{31}}\frac{1}{\tau_3 Q_{43}}\frac{1}{N_0 v}+\frac{A_{42}}{A_{31}}\frac{Q_{34}+Q_3}{Q_{43}}+\frac{A_{32}}{A_{31}}, \tag{3}$$

where Q_{34} and Q_{43} are the total (thermally averaged) cross sections for transfers $^2D_{3/2}\rightarrow{}^2D_{5/2}$ and $^2D_{3/2}\leftarrow{}^2D_{5/2}$, respectively, and Q_3 and Q_4 are the depopulation cross sections; N_0 is the density of the collision partner (ground-state atoms or molecules), and v is the average relative speed of the colliding partners. τ_3 and τ_4 are the lifetimes of the $^2D_{3/2}$ and $^2D_{5/2}$ states, respectively. Their values (397 ns for the 7^2D state and 538 ns for the 8^2D state, assuming $\tau_3=\tau_4$) were calculated from transition probabilities given by Anderson and Zilitis.[15] The ratios of Einstein A coefficients which were calculated from oscillator strengths reported by Migdalek and Baylis[16] are listed in Table I.

III. EXPERIMENTAL

The apparatus and experimental method have been fully described elsewhere.[10] Rb vapor, pure or mixed with a buffer gas, was contained in a glass fluorescence cell and was irradiated with monochromatic light pulses emitted by a N_2 laser-pumped dye laser. The resulting fluorescence was observed at right angles to the direction of excitation and was analyzed with a two-channel spectrometer and gated photon counter.

In the double-grating dye laser we utilized a mixture of Rhodamine 6G and Cresyl violet perchlorate to generate 660-nm radiation for the excitation of the 7^2D states, or Rhodamine 101 (or Rh640) to excite the 8^2D states using radiation at 641 nm. The Pyrex fluorescence cell, which was fitted with a vertical side arm containing an excess of liquid Rb metal, was mounted in a two-compartment oven with which it was possible to control separately the Rb-vapor density and the temperature of the fluorescing region. The cell was connected to a vacuum and gas-filling system by a greaseless stopcock which was closed during the actual measurements to prevent the loss of rubidium from the cell. Such an arrangement has the advantage over sealed-off cells in that it permits the cell to be evacuated between experimental runs and cleansed of gaseous impurities which inevitably tend to desorb from the cell walls and frequently are more efficient in quenching the atomic fluorescence than the buffer gases.

During the experiment with pure rubidium, the side-arm temperatures ranged from 373 to 451 K, corresponding to a pressure range 0.18—15.00 mTorr. In the experiments with buffer gases, the side-arm temperature was kept at 350±0.2 K (and the Rb-vapor pressure at about 4×10^{-5} Torr) to minimize the effects of Rb*-Rb collisions. The temperature of the cell was maintained at about 380 K to prevent condensation on the windows. The saturated rubidium-vapor pressure was determined from the lowest side-arm temperature. The temperatures were measured by several copper-constantan thermocouples at various locations on the fluorescence cell and the side arm, and recorded on a strip-chart recorder. Buffer-gas pressures were measured using a Convectron vacuum gauge which was calibrated against an MKS-Baratron 220B gauge. The gas pressures, which were corrected for transpiration where appropriate, were varied over a range 1—100 mTorr. Above 100 mTorr the fluorescent intensity ratios became insensitive to further pressure increase.

IV. RESULTS AND DISCUSSION

Equations (2) and (3) may be stated in terms of temperature and pressure in the fluorescence cell, which are directly measured during the experiments, as

$$\frac{A_{42}}{A_{31}}\left[\frac{I_B}{I_A}-\frac{A_{32}}{A_{31}}\right]^{-1}=\frac{1}{\tau}\frac{1}{Q_{34}}C\frac{\sqrt{T}}{P}+\frac{Q_{43}+Q_4}{Q_{34}}, \tag{4}$$

$$\frac{A_{31}}{A_{42}}\left[\frac{I_D}{I_C}-\frac{A_{32}}{A_{31}}\right]=\frac{1}{\tau}\frac{1}{Q_{43}}C\frac{\sqrt{T}}{P}+\frac{Q_{34}+Q_3}{Q_{43}}, \tag{5}$$

where $C=\sqrt{k\mu/8}$ and μ is the reduced mass of the collision partners. In the experiments with pure Rb vapor, P represents the Rb-vapor pressure. In this investigation we studied fine-structure mixing and quenching in the Rb 8^2D states, induced by collisions with ground-state Rb, He, Ne, Ar, Kr, and Xe atoms and N_2 molecules, and also in the 7^2D states, induced by collisions with Kr, Xe, and N_2.

Figure 2 shows plots of Eqs. (4) and (5) against $\sqrt{T}/P$ for pure Rb vapor, representing 8^2D fine-structure mixing by collisions with ground-state Rb atoms. As predicted by Eqs. (4) and (5), the plots are straight lines whose slopes give the transfer cross sections Q_{34} and Q_{43}; the quenching cross sections may be derived from the intercepts. The cross sections calculated by a least-squares analysis of the data are listed in Table II together with other recent values of ^2D mixing and quenching cross sec-

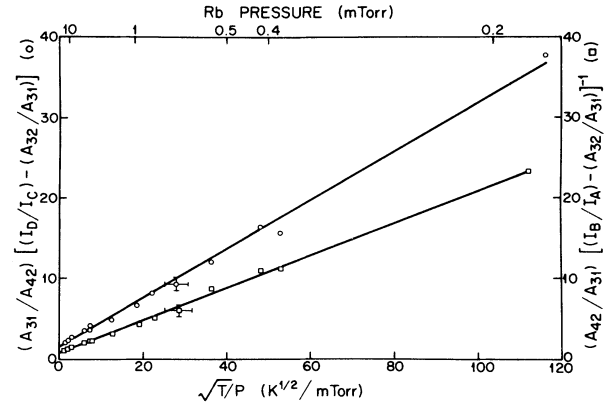

FIG. 2. Plot of the left-hand sides of Eqs. (4) and (5) against $\sqrt{T}/P$. Rough values of Rb-vapor pressures are indicated along the abscissa. The error bars are representative of experimental error over the Rb-density range.

tions for Rb*-Rb collisions. The mixing cross sections are subject to an estimated error of about 20%, arising mainly from uncertainties in the calculated values of the lifetimes and Einstein A coefficients, possible errors in the sensitivity intercalibration of the two photon-counting channels, and the uncertainty in the determination of the Rb-vapor pressure from the side-arm temperature, bearing in mind that the empirical temperature—vapor-pressure relation[19] is subject to the error inherent in the data on which it is based.

We have also considered various other possible sources of systematic error which we deem to be negligible. The effects of saturation, photoionization, and pooling collisions were all studied by measuring the intensities of the two fluorescent components as a function of laser power. At low laser powers, typical of the conditions under which the final data were taken, the intensities varied quadratically with laser power as expected from two-photon excitation, and the intensity ratio of sensitized to direct fluorescence remained constant, indicating that pooling collisions and photoionization were not significantly affecting the results. The intensities and intensity ratio deviated from this behavior only at much higher laser powers.

Collisions with Rb_2 molecules whose density was lower than the Rb density by 3 orders of magnitude would contribute negligibly to the observed effects, as would three-body collisions at the prevailing vapor densities. Blackbody radiation-stimulated transitions would cause an increase in the depopulation rate or an effective decrease in the ^2D lifetimes which, however, amounts to less than 3% of the calculated lifetimes[20] and can thus be neglected. We have also rejected the possibility of collisions with the cell walls since the fluorescing region was located at the center of the fluorescence cell which was 2.5 cm in diameter and the excited Rb atoms could travel only about 2 mm during the time of observation, even in the absence of any collisions.

It may be seen that there are differences between the values of the mixing cross section for the same transition measured in different laboratories or at different times, though there is agreement within 1 order of magnitude. We ascribe the large cross sections found by Głódź *et al.*[9] to the fact that they worked with a sealed cell and that, consequently, their results were probably perturbed by contamination adsorbed on the cell walls, in spite of the baking-out process. We have found that such gaseous impurities may considerably affect fluorescent intensity measurements, particularly at buffer-gas pressures of 1 mTorr or less. In the course of this investigation we have noted that when the stopcock on the cell was kept closed for about 1 h, there was already a change in the measured fluorescent intensity ratio at a constant (low) buffer-gas pressure. The discrepancies with the cross sections reported by Parker *et al.*[11] are more difficult to explain. For their calculations these authors used slightly different

TABLE II. Cross sections for ^2D mixing induced in Rb-Rb collisions (in units of 10^{-14} cm^2).

Rb ^2D state	ΔE fine-structure splitting (cm^{-1})	Source	Q_{34}	Q_{43}	$\frac{Q_{34}}{Q_{43}}$	Q_3	Q_4	n^*	σ_g (^2D)
5^2D	2.96	Parker *et al.*[a]		2.9± 0.6				3.71	3.14
6^2D	2.26	Hill *et al.*[b]		10±6			38±6	4.68	8.90
6^2D	2.26	Parker *et al.*[a]		6.9±1.4				4.68	8.90
7^2D	1.51	Wolnikowski *et al.*[c]	30±5	18± 3	1.65	19±6	7±2	5.67	20.3
7^2D	1.51	Parker *et al.*[a]		11.5±2.3				5.67	20.3
8^2D	1.01	Głódź *et al.*[d]	81±16	55±11	1.47	35±22	28+29	6.67	40.2
8^2D	1.01	This work	43.1± 8.6	28.5± 5.7	1.51	8±6	7±5	6.67	40.2
8^2D	1.01	Parker *et al.*[a]		17.1± 3.0				6.67	40.2
9^2D	0.70	Parker *et al.*[a]		26.0± 5.0				7.66	71.3
9^2D	0.70	Gounand *et al.*[e]	70±30			8±3		7.66	71.3

[a]Reference 11.
[b]Reference 17.
[c]Reference 10.
[d]Reference 9.
[e]Reference 18.

values of the Einstein A coefficients and much different lifetimes of the Rb ^2D states. As already stated elsewhere,[9,10] we believe that the lifetimes derived from the calculations of Anderson and Zilitis[15] are the most reliable at this time because of their agreement with other theoretical and experimental values. However, upon adjusting Parker's cross sections for the difference in lifetimes,[11] the divergencies between our results and theirs become even larger. In trying to find a rational explanation for these differences we note that, while in Ref. 11 the 6^2D mixing cross section for Rb*-Rb collisions is reported as 6.9×10^{-14} cm^2, the corresponding cross section for Rb*-Xe collisions is quoted in Ref. 12 to be 9.3×10^{-14} cm^2. In all other known cases the alkali-alkali fine-structure mixing cross section is larger than the corresponding alkali—noble-gas cross section because of the stronger dipole-dipole interaction.[1] The contrary indication given by Refs. 11 and 12 poses the question whether the authors may not have overestimated the Rb density in their system.

No theoretical calculations of Rb*-Rb cross sections for ^2D mixing have been reported in the literature but the experimental values are comparable with σ_g, the geometrical cross sections[10,21] which are also shown in Table II and which behave similarly with respect to n^*, the effective quantum number.[21] As was pointed out previously,[10,22] σ_g might be considered approximately equivalent to the sum of $Q_{43}+Q_4$, and there is agreement within experimental error between the values determined in this investigation and the calculated σ_g for the 8^2D states, as well as for the previously studied 7^2D states.[10]

The experimental data representing 7^2D and 8^2D fine-structure mixing and quenching by collisions with the noble gases and N_2 molecules are presented in Figs. 3–5, and the resulting cross sections are listed in Table III. All the plots representing Eqs. (4) and (5) are linear over the whole range of gas pressures, showing that in this particular application the Baratron is superior to the McLeod gauge which previously gave erroneous readings at the lowest densities of Ne and Ar.[10] It might be noted that the scatter of the data points corresponding to the I_B/I_A ratios is noticeably larger than the scatter of the I_D/I_C points, particularly at the lowest buffer-gas (or Rb-vapor) pressures. When $^2D_{3/2}$ is the optically populated state, the B fluorescent component consists of a mixture of direct and collisionally sensitized fluorescence and, in order that the sensitized fluorescent intensity be determined with good accuracy, its intensity should be comparable to

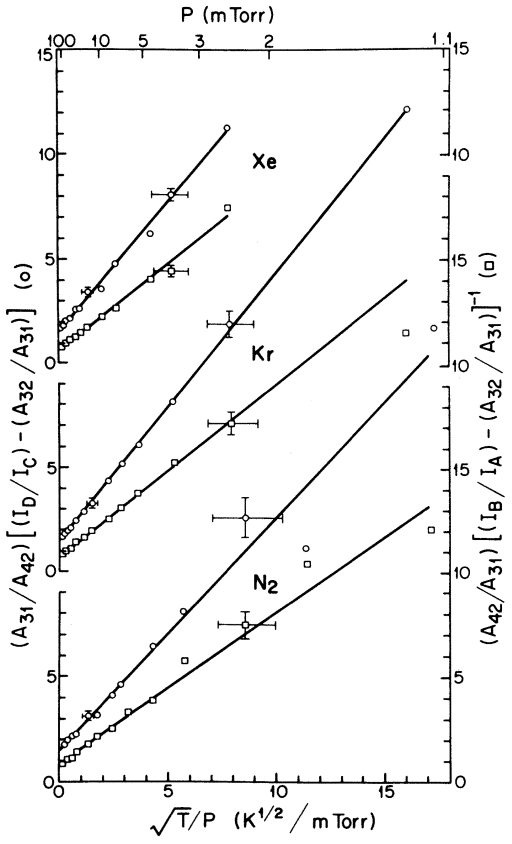

FIG. 3. Plots of the left-hand sides of Eqs. (4) and (5) against $\sqrt{T}/P$ for Kr, Xe, and N_2, showing 7^2D mixing and quenching. Rough values of gas pressures are indicated along the abscissa. The error bars are representative of experimental error over the range of gas densities.

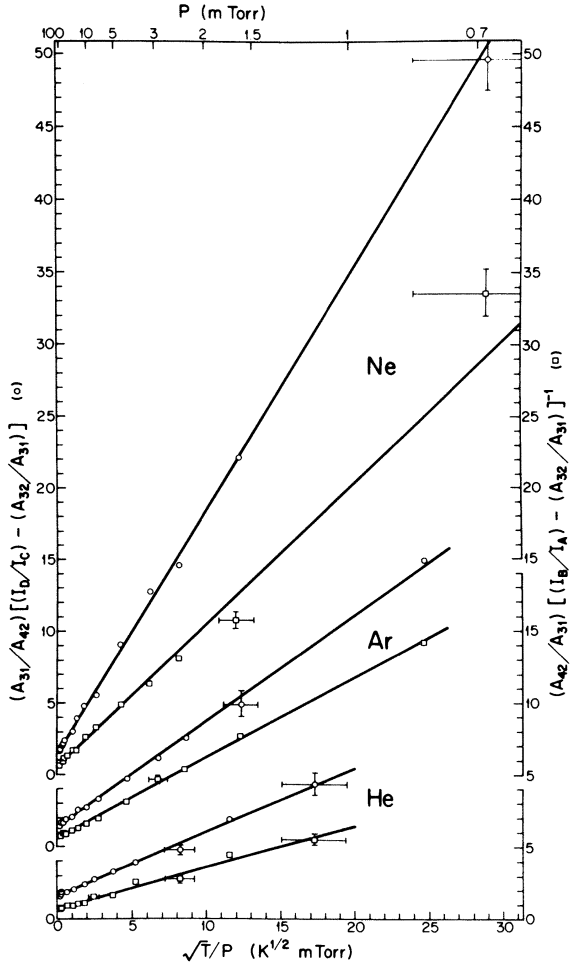

FIG. 4. Plots of the left-hand sides of Eqs. (4) and (5) against $\sqrt{T}/P$ for He, Ne, and Ar, showing 8^2D mixing and quenching.

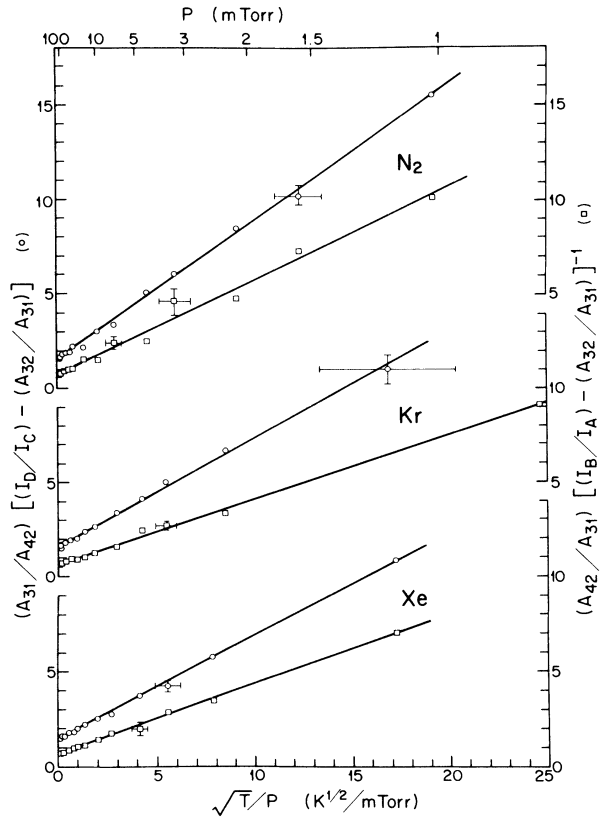

FIG. 5. Plots of the left-hand sides of Eqs. (4) and (5) against $\sqrt{T}/P$ for Kr, Xe, and N_2, showing 8^2D mixing and quenching.

the intensity of the direct fluorescence. This is accomplished only when the buffer-gas pressure exceeds some lower limit; otherwise, the experimental value of the point on the graph, representing the left-hand side of Eq. (4), becomes very sensitive to the intercalibration of the two photon-counting channels and even a small error in their relative sensitivity results in considerable scatter of the measured intensity ratios. We believe the fine-structure mixing cross sections to be accurate to within 15%. The quenching cross sections Q_3 and Q_4 are considerably less accurate; they should be regarded as a byproduct of the experiment and may, at best, be accurate within an order of magnitude. The various sources of experimental error have already been mentioned in connection with the Rb*-Rb collisions; in the present case the uncertainty in Rb density as determined from temperature—vapor-pressure relations,[19] is of no particular importance, though there is the possibility of the results being inflated through the contribution of Rb*-Rb collisions to the ^2D mixing process. At Rb-vapor densities of 1×10^{12} cm^{-3} which were employed in these experiments we found that in the most unfavorable case the necessary correction to the measured fluorescent intensity ratios did not exceed 5%.

The cross sections listed in Table III are significantly smaller than the cross sections for resonant Rb*-Rb collisions in which the interaction has a much longer range. The noble-gas cross sections for 7^2D and 8^2D mixing exhibit a pronounced minimum at Ne, which is to be expected, bearing in mind that the interaction takes place essentially between the noble-gas atom and the Rb valence electron which appears to behave as a quasi-free-particle. This relative ordering among the cross sections, which can be deduced from Omont's[23] arguments, has been observed in studies of collisional l mixing in sodium[3] and even in ^2P mixing between alkali-resonance fine-structure states,[1,24] where the valence electron would be expected to be more tightly bound. Figure 6 shows how the mixing cross sections Q_{43} vary from one noble gas to the other, with the elastic electron scattering cross sections σ[25] plotted for the sake of comparison; the atomic numbers of the noble gases serve as a convenient index. The electrons were assigned velocities equal to the appropriate ^2D orbital velocities.[21,26] It may be seen that the cross sections σ, corresponding to the 7^2D and 8^2D (and 6^2D) orbital electrons, all follow the same trend. In each case the cross section for He is larger than for Ne or Ar, and there is a minimum in the vicinity of Ne or Ar. The same trend is

TABLE III. Cross sections for ^2D mixing induced in collisions with atoms and molecules (in units of 10^{-14} cm^2).

Collision partners	Q_{34} ($^2D_{3/2}\rightarrow{}^2D_{5/2}$)	Q_{43} ($^2D_{3/2}\leftarrow{}^2D_{5/2}$)	$\frac{Q_{34}}{Q_{43}}$	Q_0 $^2D_{3/2}$	Q_0 $^2D_{5/2}$	Q(theor.)
7^2D Rb–He[a]	8.8±1.3	5.8±0.9	1.51	1.1±0.3	0.3±0.1	7.5
7^2D Rb–Ne[a]	6.5±1.0	4.0±0.6	1.62	0.2±0.1	0.2±0.1	
7^2D Rb–Ar[a]	10.4±1.6	6.9±1.0	1.50	0.1±0.1	0.5±0.5	10
7^2D Rb–Kr	14.1±1.5	9.0±1.0	1.57	0.3±0.2	0.2±0.2	
7^2D Rb–Xe	15.5±2.0	10.5±1.5	1.48	0.7±0.4	0.4±0.3	
7^2D Rb–N_2	10.0±1.5	6.9±1.0	1.45	0.8±0.4	0.3±0.3	
8^2D Rb–He	8.9±1.4	5.8±0.9	1.51	0.3±0.3	0.4±0.3	8
8^2D Rb–Ne	4.9±1.0	3.2±0.6	1.53	0.2±0.2	0.2±0.2	
8^2D Rb–Ar	12.4±2.5	9.4±1.9	1.32	0.7±0.7	0.5±0.5	12.5
8^2D Rb–Kr	24.9±5.0	15.1±3.0	1.65	0.7±0.8	0.8±1.0	
8^2D Rb–Xe	25.8±3.9	17.6±2.7	1.47	0.3±0.5	0.2±0.5	
8^2D Rb–N_2	12.1±2.4	8.3±1.7	1.46	0.7±0.6	0.3±0.4	

[a]Reference 10.

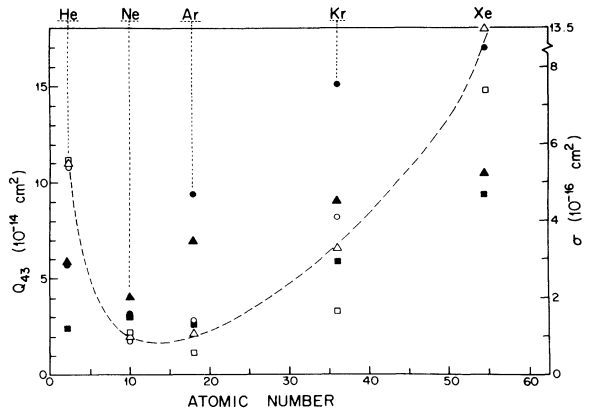

FIG. 6. Variations of cross sections Q_{43} for Rb—noble-gas collisions with the atomic numbers of the noble gases, compared with similar variations of the elastic electron scattering cross sections σ. ■, ▲, and ● represent Q_{43} for 6^2D (Ref. 12), 7^2D, and 8^2D states, respectively. □, △, and ○ represent σ corresponding to the orbital velocities of the respective ^2D electrons. The curve indicates the trend of the σ cross sections. No physical dependence of cross section on atomic number is implied.

apparent in the 7^2D and 8^2D mixing cross sections, even though they are larger than σ by 1 to 2 orders of magnitude. The 6^2D cross sections do not quite fall into this pattern; Zollars *et al.*[12] found the Ne cross section to be slightly larger than both the He and Ar cross sections. This apparently different behavior of the 6^2D cross sections might well be due to the effects of gaseous impurities adsorbed on the walls of the sealed cells, particularly at the extremely low noble-gas pressures.

The phenomenon of decreasing cross sections with increasing effective quantum number n^*, predicted by Omont,[23] may only be seen in the case of Ne which, of all the noble gases, appears to interact most weakly with Rb and thus approaches most closely Omont's postulate of "weak collisions." Although most theoretical studies of inelastic transfer cross sections apply either to the alkali-resonance states or to more highly excited Rydberg states, a useful comparison of the data for He and Ar can be made with Hahn's[27] calculation. A slight extrapolation of the curves in his Fig. 2 produces values in good agreement with the experimental values.

Table III also includes mixing and quenching cross sections for collisions with N_2. There the collisional processes might be expected to be influenced by the presence of vibrational and rotational molecular degrees of freedom. No theoretical treatments of these interactions have been reported in the literature, even though de Prunele and Pascale[7] attempted to calculate the cross sections for quenching of Na ^2D states by N_2 collisions. Their model, however, is applicable to more highly excited (Rydberg) states and produces agreement with experimental measurements only for $n > 10$. In the present case it is apparent that the cross sections for ^2D mixing by N_2 are equal to those for Ar and the respective quenching cross sections are also equal within experimental error. The equality of the mixing cross sections is not surprising. The ^2D fine-structure splittings are very much smaller than the rotational energy spacing in N_2 and thus the rotational (and vibrational) molecular degrees of freedom cannot participate in the inelastic process which otherwise would be enhanced by such a quasiresonance.[28,29] Accordingly, since N_2 has a mass and polarizability nearly equal to those of Ar, the cross sections, too, are similar. It is less obvious why the quenching cross sections should be equally similar, though the values are so inaccurate that they actually might differ by an order of magnitude. It is likely that the depopulation of the ^2D states takes place through transfer to intermediate lower-lying states, accompanied by radiative cascades, since a direct radiationless transfer to the ground state could not very well be affected by a collision with a noble-gas atom as it would involve the conversion of a large amount of excitation energy into kinetic energy of relative motion.[1] On the other hand, the N_2 quenching cross sections which lie in the range 10—100 Å^2, are close in magnitude to similar cross sections for quenching of intermediate $n\,^2P$ states in Rb[30] and Cs,[31] and ns $(5 < n < 9)$ states in Na.[14]

The principle of detailed balancing predicts that, for each ^2D state and collision partner, the mixing cross sections should be in the ratio

$$\frac{Q_{34}}{Q_{43}} = \frac{g_4}{g_3} \exp\left[\frac{-\Delta E}{kT}\right], \tag{6}$$

where $g_4 = 6$ and $g_3 = 4$ are the statistical weights of the $^2D_{5/2}$ and $^2D_{3/2}$ states, respectively, and $\Delta E \ll kT$. As may be seen in Tables II and III, all the measured ratios are quite close to the predicted value of 1.50, indicating a better internal consistency than might be expected on the basis of the probable error assigned to the individual cross sections.

ACKNOWLEDGMENT

This research was supported by the Natural Sciences and Engineering Research Council of Canada.

[1] L. Krause, in *The Excited State in Chemical Physics*, edited by J. W. McGowan (Wiley, New York, 1975).
[2] J. M. Mestdagh, J. Cuvellier, J. Berlande, A. Binet, and P. de Pujo, J. Phys. B **13**, 4589 (1980); **15**, 439 (1982).
[3] T. J. Gallagher, S. A. Edelstein, and R. M. Hill, Phys. Rev. A **15**, 1945 (1977).
[4] R. Biraben, K. Beroff, G. Grynberg, and E. Giacobino, J. Phys. (Paris) **40**, 519 (1979).
[5] M. Hugon, F. Gounand, P. R. Fournier, and J. Berlande, J. Phys. B **12**, 2707 (1979).
[6] J. Pascale and M. Y. Perrin, J. Phys. B **13**, 1839 (1979).
[7] E. de Prunelé and J. Pascale, J. Phys. B **12**, 2511 (1979).
[8] K. Sasano, Y. Sato, and M. Matsuzawa, Phys. Rev. A **27**, 2421 (1983).
[9] M. Głódź, J. B. Atkinson, and L. Krause, Can. J. Phys. **59**, 548 (1981).

[10]J. Wolnikowski, J. B. Atkinson, J. Supronowicz, and L. Krause, Phys. Rev. A **25**, 2622 (1982).
[11]J. W. Parker, H. A. Schuessler, R. H. Hill, and B. G. Zollars, Phys. Rev. A **29**, 617 (1984).
[12]B. G. Zollars, H. A. Schuessler, J. W. Parker, and R. H. Hill, Phys. Rev. A **28**, 1329 (1983).
[13]T. F. Gallagher, K. A. Safinya, and G. A. Ruff, Phys. Rev. A **27**, 2222 (1983).
[14]L. M. Humphrey, T. F. Gallagher, W. E. Cooke, and S. A. Edelstein, Phys. Rev. A **18**, 1383 (1978).
[15]F. M. Anderson and V. A. Zilitis, Opt. Spektrosk. **16**, 382 (1964) [Opt. Spectrosc. (1964) (USSR) **16**, 211 (1964)].
[16]J. Migdałek and W. E. Baylis, Can. J. Phys. **57**, 1708 (1979).
[17]R. H. Hill, H. A. Schuessler, and B. G. Zollars, Phys. Rev. A **25**, 834 (1982).
[18]F. Gounand, P. R. Fournier, and M. Hugon, *Abstracts of the Eleventh International Conference on the Physics of Electronic and Atomic Collisions, Kyoto, 1979,* edited by K. Takayanaki and N. Oda (The Society for Atomic Collision Research, Kyoto, 1979).
[19]A. N. Nesmeyanov, *Vapor Pressures of the Elements* (Academic, New York, 1963).
[20]J. W. Farley and W. H. Wing, Phys. Rev. A **23**, 2397 (1981).
[21]H. Bethe and E. E. Salpeter, Handb. Phys. **35**, 88 (1955).
[22]M. Hugon, F. Gounand, and P. R. Fournier, J. Phys. B **13**, L109 (1980).
[23]A. Omont, J. Phys. (Paris) **38**, 1343 (1977).
[24]J. Ciuryło and L. Krause, J. Quant. Spectrosc. Radiat. Transfer **28**, 457 (1982).
[25]H. S. W. Massey and E. H. S. Burhop, *Electronic and Ionic Impact Phenomena, Vol. I* (Clarendon, Oxford, 1952).
[26]B. Pitre, A. G. A. Rae, and L. Krause, Can. J. Phys. **44**, 731 (1966).
[27]Y. Hahn, J. Phys. B **14**, 985 (1981).
[28]J. Cuvellier, J. M. Mestdagh, M. Ferray, and P. de Pujo, J. Chem. Phys. **79**, 2848 (1983).
[29]E. S. Hrycyshyn and L. Krause, Can. J. Phys. **48**, 2761 (1970).
[30]I. N. Siara and L. Krause, Can. J. Phys. **51**, 257 (1973).
[31]I. N. Siara, R. U. Dubois, and L. Krause, Can. J. Phys. **60**, 239 (1982).